SVM Strategies for Multiphase Voltage Source Inverters

Zipan Nie*, Matthias Preindl†, Nigel Schofield†††

**McMaster University, Canada, niez4@mcmaster.ca, †McMaster University, Canada, preindl@mcmaster.ca, †††McMaster University, Canada, nigels@mcmaster.ca*

Keywords: Space Vector Modulation (SVM), Voltage Source Inverter (VSI), multiphase, Vector Space Decomposition (VSD), Brushless Permanent Magnet (BLPM) Machine

Abstract

This paper compares Space Vector Modulation (SVM) strategies for multiphase inverters. Symmetric, discontinuous, and group-based SVM and Sinusoidal Pulse Width Modulation (SPWM) are compared against each other. Implementation techniques for *n*-phase modulation are discussed using the Vector Space Decomposition (VSD) and a direct approach using inverse Clarke transformation including harmonic injection. The modulation techniques are validated experimentally using a 3-phase and 9-phase brushless permanent magnet (BLPM) machine drive system.

1 Introduction

Electric machine drive systems of different power range have been applied in different fields: hybrid/full electrical vehicles [1,2], aerospace actuators and generation systems [2,3], traction systems on 'more electrical ship' [4,5] and so on. Industrial variable speed, AC electric drive systems have gained application track record over the last 20 years, a market sector that seems to be increasing in size and displacing traditional fixed supply and speed electric drives due to established improvements in drive system energy conversion efficiency and functionality. These systems are essentially 3-phase; however, the traditional 3-phase system has some shortcomings. Particularly where fault tolerance is a specific requirement and in high power (~100 kW upwards), where high current switching devices are required due to the high power (current) per phase. Hence, AC drive systems with more than 3-phases have been proposed e.g. for aerospace applications where fault tolerance is critical [2,3]. Moreover, even in applications where 3-phase systems are fully capable, the multiphase AC drive system can be competitive and may improve existing systems.

The comparisons between normal 3-phase and multiphase machine drive systems indicate that the application of multiphase machine and power electronic inverter can reduce the power handling and hence rating per phase [6], increase the fault tolerance capability [7], and improve the torque output [1]. Detailed comparison between 3-phase and 9-phase brushless permanent magnet (BLPM) machine drive systems [1,8] gives a general view and quantitative analysis and evaluation between them. Under the conditions that the stator current density and machine geometry are the same, the application of 9-phase BLPM drive system improves the torque capability and torque quality, decreases the iron losses, and the inverter DC-link voltage ripple, thus reducing the drive system smoothing capacitor [8]. Due to their advantages in some applications, 9-phase and other multiphase machine drive systems are worthy of study hence the consideration of this paper.

With the increase of phase number, the switching strategies for multiphase inverters become more complex. Generally, a Vector Space Decomposition (VSD) approach is taken [2] wherein the most widely used switching strategies are Carrier-based Pulse Width Modulation (CBPWM) [2,3,9-12] and Space Vector Modulation (SVM) [2,5,6,9,12-17]. Although CBPWM with fundamental and certain harmonics injection can improve the DC-bus utilization comparing with Sinusoidal Pulse Width Modulation (SPWM) [4], SVM has better DC-bus utilization if only large, i.e. group D vectors, are applied, where the vector groups are discussed later in Section 3.

SVM strategies have been discussed for 9-phase voltage source inverters and tested using simple resistive-inductive loads [15] and induction machines [16]. This paper validates multiphase SVM for BLPM drive systems. So far, only one type of SVM has been investigated for 9-phase systems [15,16], here the authors only use – selected active voltage vectors, and there is no comparison with other SVM strategies. Moreover, there has been no solution to generalize the SVM strategy for *n*-phase systems.

This paper presents the solution for a generalized SVM strategy for *n*-phase drive systems and applies it to a 9-phase BLPM drive system. Four different SVM strategies containing (i) symmetrical SVM, (ii) discontinuous SVM, (iii) group based 3x 3-phase SVM and (iv) selective active voltage vector SVM (only the largest voltage vectors employed), are implemented to switch a 9-phase voltage source inverter (VSI) controlling a BLPM drive system; to evaluate and compare their corresponding performances via simulations and experiments. A single fundamental CBPWM, i.e. SPWM strategy, is also implemented experimentally as a benchmark reference.

2 Generalized multiphase system stationary coordinate transformation

The VSD approach has been introduced to model and analyse multiphase systems [2]. An *n*-phase system can be decomposed into a set of zero-sequence planes and *k* mutually orthogonal planes where *k* is given by:

$$k = \left\lfloor \frac{(n-1)}{2} \right\rfloor \tag{1}$$

Clarke's decoupling transformation matrix [2] for a multiphase system with an arbitrary phase number *n* is shown in Equation (2). The first two rows correspond to the 1st plane (alpha-beta plane) of this multiphase system and define the fundamental component. The last two rows correspond to the k^{th} plane and define the zero-sequence components. An odd number phase system with star connection topology and a floating neutral point does not contain any of the zero-sequence components. While an even number phase system contains one 0_- component [2]. Different planes define different order harmonics, i.e.:

x_1-y_1 plane: $nh \pm 1$ harmonics (where h is even)
x_2-y_2 plane: $nh \pm 2$ harmonics (where h is odd)
…
x_k-y_k plane: $nh \pm k$ harmonics (where h is odd when k is odd, h is even when k is even)

$$C = m \cdot \begin{bmatrix} 1 & \cos\alpha & \cos 2\alpha & \cos 3\alpha & \cdots & \cos 3\alpha & \cos 2\alpha & \cos\alpha \\ 0 & \sin\alpha & \sin 2\alpha & \sin 3\alpha & \cdots & -\sin 3\alpha & -\sin 2\alpha & -\sin\alpha \\ 1 & \cos 2\alpha & \cos 4\alpha & \cos 6\alpha & \cdots & \cos 6\alpha & \cos 4\alpha & \cos 2\alpha \\ 0 & \sin 2\alpha & \sin 4\alpha & \sin 6\alpha & \cdots & -\sin 6\alpha & -\sin 4\alpha & -\sin 2\alpha \\ \vdots & \vdots & \vdots & \vdots & \cdots & \vdots & \vdots & \vdots \\ 1 & \cos k\alpha & \cos 2k\alpha & \cos 3k\alpha & \cdots & \cos 3k\alpha & \cos 2k\alpha & \cos k\alpha \\ 0 & \sin k\alpha & \sin 2k\alpha & \sin 3k\alpha & \cdots & -\sin 3k\alpha & -\sin 2k\alpha & -\sin k\alpha \\ 1/\sqrt{2} & 1/\sqrt{2} & 1/\sqrt{2} & 1/\sqrt{2} & \cdots & 1/\sqrt{2} & 1/\sqrt{2} & 1/\sqrt{2} \\ 1/\sqrt{2} & -1/\sqrt{2} & 1/\sqrt{2} & -1/\sqrt{2} & \cdots & -1/\sqrt{2} & 1/\sqrt{2} & -1/\sqrt{2} \end{bmatrix} \begin{matrix} x_1 \\ y_1 \\ x_2 \\ y_2 \\ \vdots \\ x_k \\ y_k \\ 0_+ \\ 0_- \end{matrix} \tag{2}$$

where $\alpha = 2\pi / n$

In a *n*-phase system the total instantaneous power:

$$P_{abcd\cdots} = \left[V_{abcd\cdots}\right]^T \left[I_{abcd\cdots}\right] \tag{3}$$

In *k* planes the total power is:

$$\begin{aligned} P_{x1y1x2y2\cdots} &= \left[V_{x1y1x2y2\cdots}\right]^T \left[I_{x1y1x2y2\cdots}\right] \\ &= \left[V_{abcd\cdots}\right]^T C^T C \left[I_{abcd\cdots}\right] \end{aligned} \tag{4}$$

Under the power-invariant conditions, the factor *m* can be derived from:

$$m = \sqrt{\frac{2}{n}} \tag{5}$$

while under the amplitude-invariant conditions, the factor *m* can be derived from:

$$m = \frac{2}{n} \tag{6}$$

The following discussion focuses on the voltage and current waveforms and hence the amplitude-invariant Clarke transformation is used.

In most BLPM drive system situations, the machine inverter needs to output sinusoidal current waveforms such that the stator flux matches the rotor induced sinusoidal back-EMF. Only the fundamental component of phase current contributes to the steady output torque and thus the analysis in the first plane is enough for the fundamental output, while the harmonics from the other planes can result in stator flux distortion in the machine air gap. Consequently, in this paper the analysis will be mainly based on the first plane.

3 SVM strategies

In a two level multiphase VSI there are *n* legs, 2*n* switches, and 2^n different switching states i.e. voltage vectors. Each phase can be represented by a series connected resistor, inductor, and voltage source (machine back-EMF). Different SVM strategies are discussed in this Section using a 9-phase BLPM as an example. The machine phases form a 9-phase star that can also be separated into 3x 3-phase star points. Hence there is one neutral point for the 9-phase system and 3 neutral points for the 3x 3-phase configuration, as shown in Figure 1.

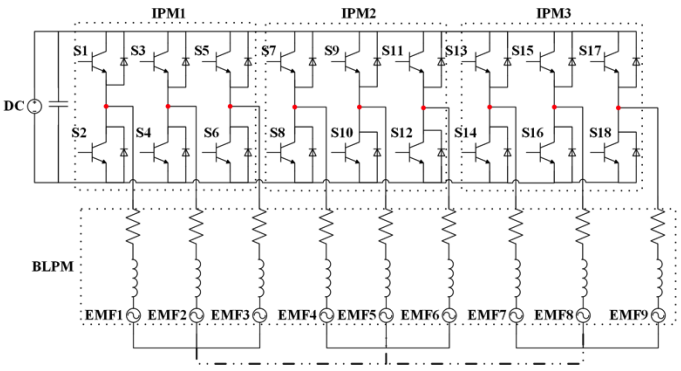

Figure 1: 9-phase VSI and BLPM.

3.1 SVM with selected voltage vectors

For a *n*-phase system with one group of voltage vectors employed SVM strategies, the stationary coordinate (first plane) is divided into 2*n* sections, in which the reference voltage vector is synthesized by the neighbourhood two vectors, and their operating time and zero time in each switching period are given by Equations (7) (8), (9) and illustrated in Figure 2(a), with the exception of over modulation operation. Specific to the 9-phase application, *n* is equal to 9. For 3-phase SVM there is only one group of 6 voltage vectors with the same magnitude and 2 zero vectors.

$$T_N = \frac{T_c U_{x1} \sin\left[N\left(180^\circ / n\right)\right] - T_c U_{y1} \cos\left[N\left(180^\circ / n\right)\right]}{\left|\vec{V}_N\right| \sin\left(180^\circ / n\right)} \tag{7}$$

$$T_{N+1} = \frac{T_c U_{x1} \sin\left[(N-1)\cdot\left(180^\circ / n\right)\right] - T_c U_{y1} \cos\left[(N-1)\cdot\left(180^\circ / n\right)\right]}{-\left|\vec{V}_{N+1}\right| \sin\left(180^\circ / n\right)} \tag{8}$$

$$T_0 = T_c - T_N - T_{N+1} \tag{9}$$

where *N* is the sector number (from 1 to 2n), T_c is the switching period, U_{x1} and U_{y1} are the voltage vector variables in stationary coordinates, $\vec{V}_N$ and $\vec{V}_{N+1}$ are two neighbourhood active voltage vectors and T_N T_{N+1} and T_0 are the respective application times for two active voltage vectors and zero vectors.

Taking the 9-phase system for example; at any instance, *M* upper switches and corresponding (9-*M*) lower switches are switched on, which leads to voltage vectors with different DC

bus utilization. The highest DC bus utilization voltage vectors are selected in each combinations with different *M* and categorized into four groups:

- Group A: 1 or 8 upper switches ON
- Group B: 2 or 7 upper switches ON
- Group C: 3 or 6 upper switches ON
- Group D: 4 or 5 upper switches ON

Comparison has been made for different voltage vector groups in terms of the ratio between their magnitudes and the DC bus voltage as shown in Figure 2(b). In each switching period up to 8 active voltage vectors can be employed to generate the reference voltage vector. In some situations, all the voltage vectors are applied [5,15] while in other situations, only one group of the voltage vectors with the biggest magnitudes are introduced [5]. In terms of switching events number (corresponding to the switching losses), modulation index, and control complexity, the scheme with only one group of active voltage vectors has its advantage.

The employment of different groups of active voltage vectors results in different performances. To achieve maximum drive capability only group D is selected. However, this approach does not apply a given or even known voltage in the x2y2, x3y3, etc. planes, in which these "parasitic" voltages will drive unintended current harmonics.

Another scenario to achieve *n*-phase SVM is to apply group based SVPWM. For an arbitrary *n*-phase system, if *n* is a multiple of 3, this system can be composed of (*n*/3)x 3-phase systems. The same approach is also eligible if *n* is a multiple of 5, 7 etc. Then the system can be composed of multiple 5-phase, 7-phase systems etc. For a symmetrical 9-phase system, the phase shift between two consecutive voltage phases is 40º electrical, while in a 3-phase system it is 120º electrical. As a consequence, a 9-phase system can be composed of 3x 3-phase systems shifted by 40º electrical, as shown in Figure 2(c), in which each 3-phase inverter is controlled by 3-phase SVM. Under this condition the machine has three separate floating neutral points. From phase current and voltage view, this switching modulation scheme is inherently a 3-phase SVM.

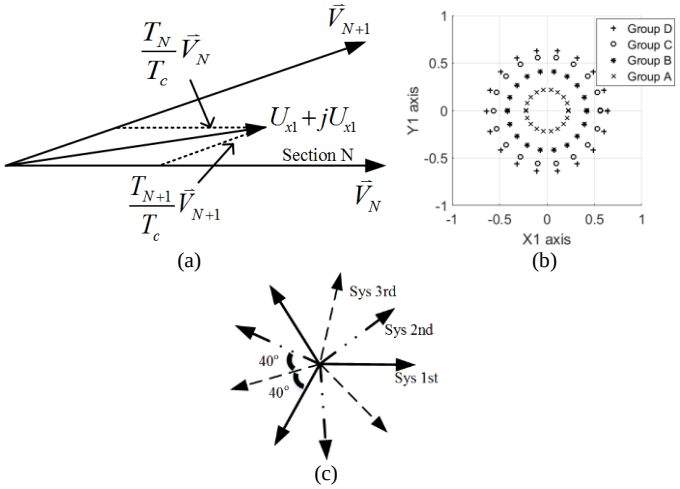

Figure 2: SVM voltage vectors synthesis, different groups of voltage vectors, and group-based SVM.

3.2 Symmetrical and discontinuous SVM based on inversion of the Clarke transformation

VSD approach is used here to only enable the first plane output and set the other planes x2y2, x3y3 etc. to zero. Another scheme to achieve *n*-phase SVM is to implement zero sequence injection on SPWM, which has the equivalent performance with the SVM with all the possible voltage vectors employed. This scheme has been implemented in a 3-phase system [18-20] and here it is generalized to *n*-phase system SVM solution. Two different strategies, symmetric SVM and discontinuous SVM are discussed here.

In SPWM *n*-phase duty ratios are $d_{SPWM}(1)$ to $d_{SPWM}(n)$, where the maximum and minimum values are deduced from:

$$d_{\max} = \max\left[d_{SPWM}(1) \quad d_{SPWM}(2) \quad \cdots \quad d_{SPWM}(n)\right] \tag{10}$$

$$d_{\min} = \min\left[d_{SPWM}(1) \quad d_{SPWM}(2) \quad \cdots \quad d_{SPWM}(n)\right] \tag{11}$$

For *n*-phase symmetric SVM the phase *n* duty ratio is:

$$d_{SVM}(n) = d_{SPWM}(n) + 0.5\cdot(1 - d_{\max} - d_{\min}) \tag{12}$$

For *n*-phase discontinuous SVM the phase n duty ratio is:

$$d_{DSVM}(n) = \begin{cases} d_{SPWM}(n) - d_{\min} & d_{\max} + d_{\min} < 1 \\ d_{SPWM}(n) + (1 - d_{\max}) & d_{\max} + d_{\min} \geq 1 \end{cases} \tag{13}$$

Phase voltage duty ratios for 3-phase and 9-phase systems are presented in Figure 3.

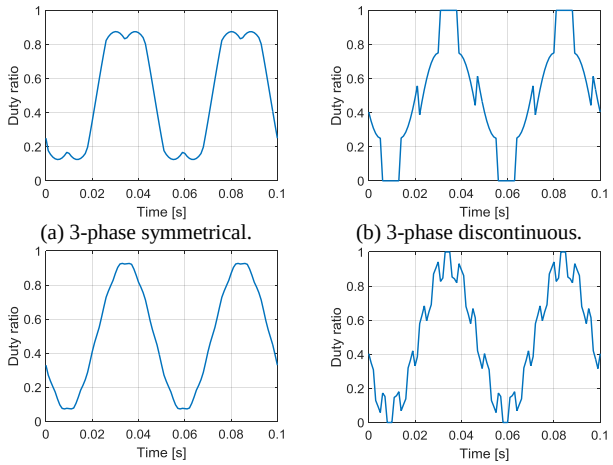

Figure 3: Duty ratios for 3-phase and 9-phase systems.

The maximum modulation index is defined here as the ratio between output phase-to-neutral voltage (peak) of the fundamental component and the DC-link voltage except for when the inverter is over modulated. Table 1 shows the maximum modulation index (MMI) that can be achieved by different modulation strategies. It is noted that SVM with selected voltage vectors can achieve the highest MMI that is achieved by applying voltages in the x2y2, x3y3 and x4y4 planes that drive undesired currents.

4 Simulation and experiment results

Simulations are conducted to analyse, compare and evaluate different SVM strategies with the consideration of their Total Harmonic Distortion (THD) and harmonics spectra of phase-to-neutral voltage and current. SPWM strategy is also simulated here as a benchmark for comparison.

The test machine has a concentrated coil winding per phase, each phase having a phase resistance of 1.7ohms and phase self-inductance of 4.3mH. In the simulation, mutual inductance is neglected and the back-EMF is modelled as a voltage source (the sum of fundamental and 3rd harmonic) with certain phase shift to the phase voltage. The simulations are conducted with the following conditions: (i) DC-bus voltage=80V, (ii) switching frequency=5kHz, (iii) fundamental output frequency=20Hz and the fundamental phase voltage 8=Vpeak.

Number of phases n	Sinusoidal PWM	Symmetric/ discontinuous SVM	SVM with selected voltage vectors
3	0.5	0.5775	0.5775
4		0.5000	0.5000
5		0.5255	0.6155
6		0.5000	0.5775
7		0.5130	0.6260
8		0.5000	0.6035
9		0.5075	0.6300
10		0.5000	0.6155
∞		0.5000	0.6365

Table 1: Comparisons of Maximum modulation index.

Four SVM strategies containing 9-phase SVM symmetrical, 9-phase SVM discontinuous, 9-phase SPWM (benchmark) and 3x 3-phase SVM, are implemented with the experimental setup composed of a TMS320F28377D DSP as the controller, 3 PM50RLA060 intelligent power modules (IGBT with 3-phase full bridges) from Powerex and their corresponding driver boards Powerex BP7B, Hengstler incremental encoder RS58-D/5000AD.37RB, power supplies and accessary circuit boards for logical signal conversion and protection. In terms of the measurement, a Tektronix oscilloscope MDO3024, Metrix differential probe MX 9003, and LEM LA 55-P current transducer are used to capture the voltage and current waveforms. The experimental setup is shown in Figure 4. Experiments are conducted here under the same conditions with the simulations to validate these SVM strategies.

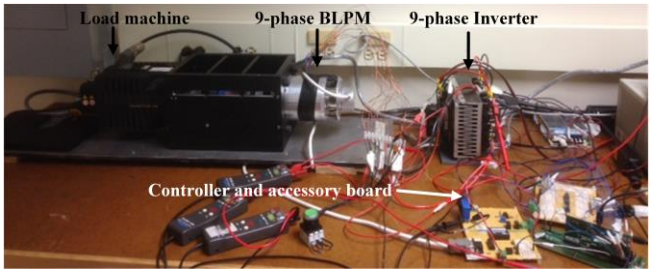

Figure 4: Experiment setup.

Figure 5 shows phase 1 current and voltage waveforms from both simulations and experiments in which the distortion of phase current can be roughly compared between different strategies. To analyse the phase 1 voltage harmonic contents, Fast Fourier Transform (FFT) with the consideration between 0Hz to 25kHz is implemented and the voltage spectra results are shown in Figure 6. Phase 1 current and voltage THD are shown in Table 2.

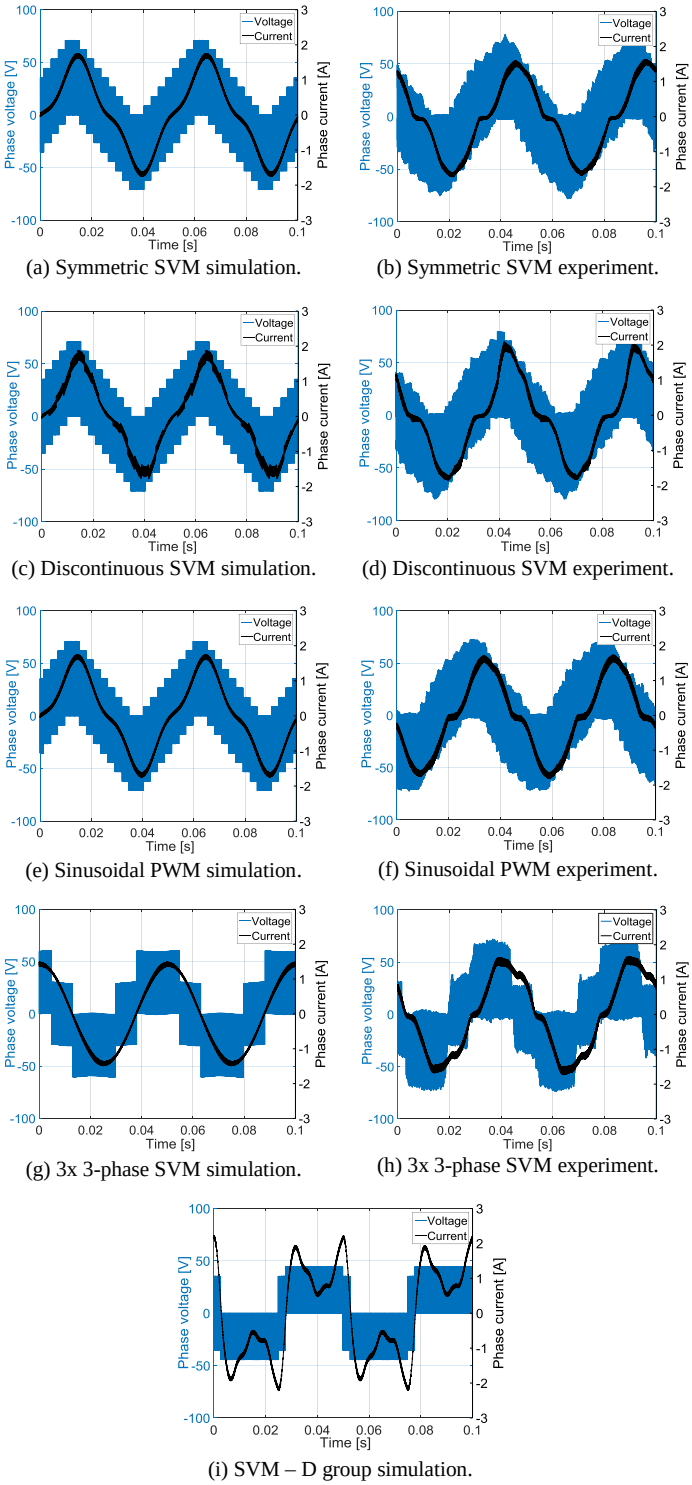

(a) Symmetric SVM simulation.
(b) Symmetric SVM experiment.
(c) Discontinuous SVM simulation.
(d) Discontinuous SVM experiment.
(e) Sinusoidal PWM simulation.
(f) Sinusoidal PWM experiment.
(g) 3x 3-phase SVM simulation.
(h) 3x 3-phase SVM experiment.
(i) SVM – D group simulation.

Figure 5: Phase 1 voltage and current waveforms from different switching schemes employed.

From Figure 5, and Figure 6 the experiment results show good agreement with the simulation results. However, there are some slight differences between them because: (i) the machine back-EMF has some higher order harmonics although these are of very low magnitude. (ii) there is some fluctuation on the experimental DC-bus due to the input rectification stage and (iii) the switching dead time (2μs) is not modelled in simulation.

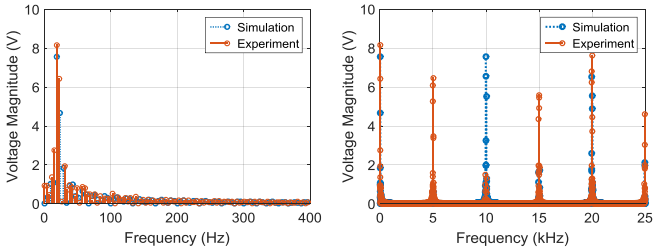

(a) Symmetric SVM.

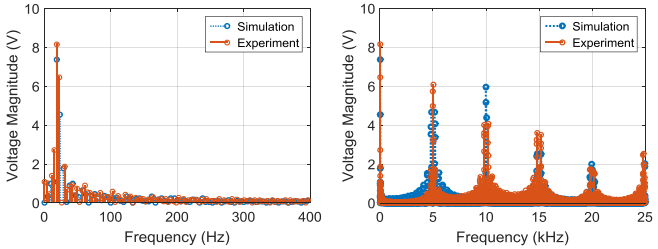

(b) Discontinuous SVM.

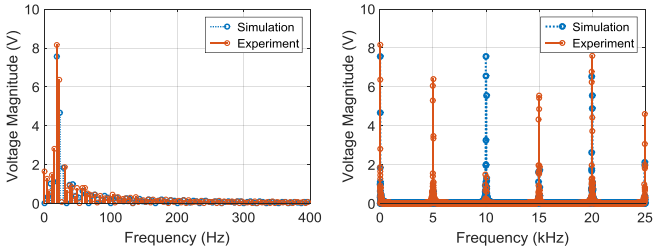

(c) Sinusoidal PWM.

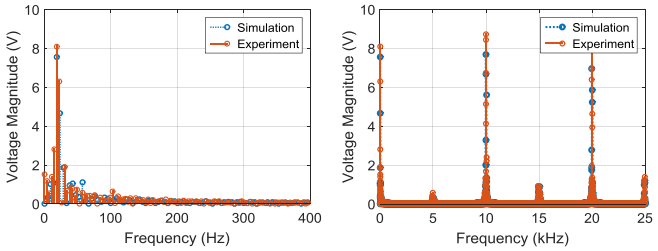

(d) 3x 3-phase SVM.

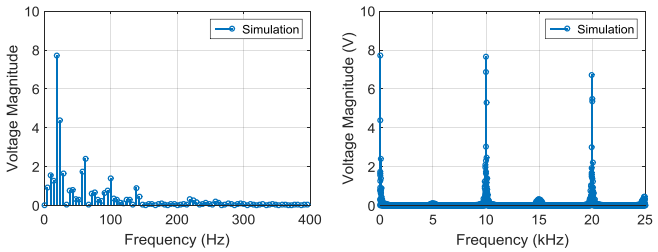

(e) SVM – D group.

Figure 6: Phase 1 voltage spectra from simulation and experimental results.

Simulations show that selective active vector SVM strategy, group D, has the highest phase voltage harmonic contents over low frequency range from 0Hz to 400Hz, i.e. 1st, 3rd, 5th, and 7th harmonics are visible in Figure 6(e), which also results in the highest phase current distortion and current THD (85.3%). This is because this strategy drives currents in the x2y2, x3y3, and x4y4 planes. As a result, no further experimental validation is conducted for this strategy because it is not an optimum considering output torque quality.

	Experiment		Simulation	
	Current THD	Voltage THD	Current THD	Voltage THD
Symmetric SVM	18.7%	270.0%	20.7%	264.6%
Discontinuous SVM	26.4%	271.0%	21.6%	265.1%
Sinusoidal PWM	20.1%	271.3%	20.4%	264.7%
3X3-phase SVM	14.2%	267.4%	3.3%	269.6%
SVM - group D	N/A	N/A	85.3%	260.3%

Table 2: Comparison between different switching schemes.

Low order voltage harmonics like 3rd, 5th, 7th relating to low frequency torque vibration are important considerations in output torque quality and copper losses in machines. Within the low frequency range 0–400Hz, SVM - group D, Figure 6(e), has the highest 3rd, 5th, 7th harmonics among these strategies. Symmetric SVM, Figure 6(a), Sinusoidal PWM, Figure 6(c), and 3x 3-phase SVM, Figure 6(d), have similar performance, while all are better than Discontinuous SVM, Figure 6(b).

High order voltage harmonics around and above the switching frequency contribute more on machine iron losses and should be taken into consideration. A 5kHz harmonic can be significantly higher dependent on the modulation index. Over the frequency range 0 – 25 kHz, discontinuous SVM has a higher noise floor and side-band sub-harmonic voltage spectrum, as shown in Figure 6(b), while symmetrical SVM and SPWM have similar contents. The 3x 3-phase SVM, Figure 6(d), shows the best harmonic content among these strategies.

In Table 2, voltage THD also shows the advantage of 3x 3-phase SVM over Symmetric SVM, Discontinuous SVM, and Sinusoidal PWM. A similar trend occurs in the current THD where 3x 3-phase SVM has the best performance.

5 Conclusions

Generalized *n*-phase system SVM strategies are introduced in this paper and implemented and validated via a 9-phase VSI and BLPM drive system. Their performances have been analysed, evaluated and compared via simulations and experiments. Among this strategies, 3x 3-phase SVM has the best performance with the compromise of voltage harmonic contents, current/voltage THD (14.2% and 267.4% respectively), and modulation index (0.578). Following are

Symmetric SVM (modulation index 0.508) which has less harmonic content in both the low and high frequency range than Discontinuous SVM. However, Discontinuous SVM has less switching events (relating to switching losses) than Symmetrical SVM. That is a trade-off between the power losses in the inverter and machine. These strategies can achieve improved torque output than SVM - group D which, despite its highest maximum modulation index (0.63), has much higher harmonic content in the low frequency range and current THD, resulting in higher torque ripple and machine copper losses.

Acknowledgements

The authors acknowledge the Canada Excellence Research Chairs (CERC) program, Natural Sciences and Engineering Research Council of Canada (NSERC) Automotive Partnership Canada (APC) for support of Mr. Nie's Ph.D. Studentship.

References

[1] N. Schofield, X. Niu, and O. Beik, "Multiphase machines for electric vehicle traction," in *Transportation Electrification Conference and Expo (ITEC), 2014 IEEE*, 2014, pp. 1–6.

[2] E. Levi, R. Bojoi, F. Profumo, H. A. Toliyat, and S. Williamson, "Multiphase induction motor drives - a technology status review," *Electr. Power Appl. IET*, vol. 1, no. 4, pp. 489–516, Jul. 2007.

[3] S. Karugaba and O. Ojo, "A carrier-based PWM modulation technique for balanced and unbalanced reference voltages in multiphase voltage-source inverters," *IEEE Trans. Ind. Appl.*, vol. 48, no. 6, pp. 2102–2109, 2012.

[4] A. Iqbal, E. Levi, M. Jones, and S. N. Vukosavic, "Generalised Sinusoidal PWM with Harmonic Injection for Multi-Phase VSIs," in *Power Electronics Specialists Conference, 2006. PESC '06. 37th IEEE*, 2006, pp. 1–7.

[5] A. Iqbal and E. Levi, "Space vector modulation schemes for a five-phase voltage source inverter," in *Power Electronics and Applications, 2005 European Conference on*, 2005, p. 12 pp.–P.12.

[6] D. Casadei, D. Dujic, E. Levi, G. Serra, A. Tani, and L. Zarri, "General Modulation Strategy for Seven-Phase Inverters With Independent Control of Multiple Voltage Space Vectors," *Ind. Electron. IEEE Trans.*, vol. 55, no. 5, pp. 1921–1932, May 2008.

[7] L. Parsa and H. A. Toliyat, "Fault-tolerant five-phase permanent magnet motor drives," in *Industry Applications Conference, 2004. 39th IAS Annual Meeting. Conference Record of the 2004 IEEE*, 2004, vol. 2, pp. 1048–1054 vol.2.

[8] A. S. Al-Adsani and N. Schofield, "Comparison of three- and nine-phase hybrid permanent magnet generators," in *Industrial Electronics, 2009. IECON '09. 35th Annual Conference of IEEE*, 2009, pp. 3880–3885.

[9] L. Zarri, M. Mengoni, A. Tani, G. Serra, and D. Casadei, "Minimization of the Power Losses in IGBT Multiphase Inverters with Carrier-Based Pulsewidth Modulation," *Ind. Electron. IEEE Trans.*, vol. 57, no. 11, pp. 3695–3706, Nov. 2010.

[10] A. Iqbal and S. Moinuddin, "Comprehensive relationship between carrier-based PWM and space vector PWM in a five-phase VSI," *IEEE Trans. Power Electron.*, vol. 24, no. 10, pp. 2379–2390, 2009.

[11] O. Ojo and G. Dong, "Generalized Discontinuous Carrier-based PWM Modulation Scheme For Multi-phase Converter-machine Systems," *Fourtieth IAS Annu. Meet. Conf. Rec. 2005 Ind. Appl. Conf. 2005.*, vol. 2, pp. 1374–1381, 2005.

[12] D. Dujic, E. Levi, M. Jones, G. Grandi, G. Serra, and a. Tani, "Continuous PWM techniques for sinusoidal voltage generation with seven-phase voltage source inverters," *PESC Rec. - IEEE Annu. Power Electron. Spec. Conf.*, pp. 47–52, 2007.

[13] D. Dujic, M. Jones, E. Levi, J. Prieto, and F. Barrero, "Switching Ripple Characteristics of Space Vector PWM Schemes for Five-Phase Two-Level Voltage Source Inverters - Part 1: Flux Harmonic Distortion Factors," *Ind. Electron. IEEE Trans.*, vol. 58, no. 7, pp. 2789–2798, Jul. 2011.

[14] M. Jones, D. Dujic, E. Levi, J. Prieto, and F. Barrero, "Switching ripple characteristics of space vector PWM schemes for five-phase two-level voltage source inverters - Part 2: Current ripple," *IEEE Trans. Ind. Electron.*, vol. 58, no. 7, pp. 2799–2808, 2011.

[15] D. Dujic, M. Jones, and E. Levi, "Space vector PWM for nine-phase VSI with sinusoidal output voltage generation: Analysis and implementation," *IECON Proc. (Industrial Electron. Conf.*, pp. 1524–1529, 2007.

[16] J. W. Kelly, E. G. Strangas, and J. M. Miller, "Multiphase space vector pulse width modulation," *Energy Conversion, IEEE Trans.*, vol. 18, no. 2, pp. 259–264, Jun. 2003.

[17] Y. Zhao and T. A. Lipo, "Space vector PWM control of dual three-phase induction machine using vector space decomposition," *Ind. Appl. IEEE Trans.*, vol. 31, no. 5, pp. 1100–1109, Sep. 1995.

[18] J.-S. Kim and S.-K. Sul, "A Novel Voltage Modulation Technique of the Space Vector PWM," *電気学会論文誌 D ('Proceedings of Electrical Engineering Institute D' in Japanese)*, vol. 116, no. 8, pp. 820–825, 1996.

[19] D.-W. Chung, J.-S. Kim, and S.-K. Sul, "Unified voltage modulation technique for real-time three-phase power conversion," *Ind. Appl. IEEE Trans.*, vol. 34, no. 2, pp. 374–380, Mar. 1998.

[20] M. Preindl, "Novel Model Predictive Control of a PM Synchronous Motor Drive; Design of the Innovative Structure, Feasibility and Stability Analysis, Efficient Implementation, Experimental Validation,", *Ph.D. Thesis*, University of Padua, Italy, 2014.